Temperature-dependent Raman scattering of DyScO$_3$ and GdScO$_3$ single crystals

Temperature-dependent Raman scattering of DyScO$_3$ and GdScO$_3$ single crystals

O Chaix-Pluchery[1], D Sauer and J Kreisel

Laboratoire des Matériaux et du Génie Physique, CNRS UMR 5628, Grenoble Institute of Technology, Minatec, 3, parvis Louis Néel, 38016 Grenoble, France

E-mail: Odette.Chaix@grenoble-inp.fr

Abstract
We report a temperature-dependent Raman scattering investigation of DyScO$_3$ and GdScO$_3$ single crystals from room temperature up to 1200 °C. With increasing temperature, all modes decrease monotonically in wavenumber without anomaly, which attests to the absence of a structural phase transition. The high temperature spectral signature and extrapolation of band positions to higher temperatures suggest a decreasing orthorhombic distortion towards the ideal cubic structure. Our study indicates that this orthorhombic-to-cubic phase transition is close to or higher than the melting point of both rare-earth scandates ($\cong$2100 °C), which might exclude the possibility of the experimental observation of such a phase transition before melting. The temperature-dependent shift of Raman phonons is also discussed in the context of thermal expansion.

(Some figures in this article are in colour only in the electronic version)

1. Introduction

The understanding of ABO$_3$ perovskite-type oxides is a very active research area with great relevance to both fundamental- and application-related issues, particularly related to dielectric and ferroelectric properties [1, 2]. The ideal cubic structure of ABO$_3$ perovskites is rather simple, with corner-linked anion octahedra BO$_6$, the B cations at the centre of the octahedra and the A cations in the space between the octahedra. With respect to this ideal cubic perovskite, structural distortions can be described by separating two main features [3–5]: (i) a rotation (tilt) of essentially rigid BO$_6$ octahedra and/or (ii) polar cation displacements. Past investigations of these instabilities have been a rich source for providing understanding of structural properties not only in perovskites but also in oxides in general.

In this paper we will focus on perovskites which present no cation displacement but only the anti-ferrodistortive (AFD) tilt distortion. It is well known [6] that this tilt distortion (the tilt angle) can be driven by external parameters such as temperature or pressure as exemplified in the model materials SrTiO$_3$ (STO) [7, 8] or LaAlO$_3$ (LAO) [9, 10]. While it has been shown that *pressure* can either increase [11] or reduce [10, 12, 13] AFD instabilities at the zone boundary, it

is generally accepted that *temperature* reduces tilt instabilities, i.e. the angle of tilt away from the cubic structure decreases with increasing temperature. However, the critical temperature T_c at which the structure becomes cubic can greatly vary (e.g. $T_{c,STO} = -163$ °C and $T_{c,LAO} = 527$ °C) [7, 9] and some tilted perovskites decrease in tilt angle but do not become cubic before their melting.

Our present work focuses on two rare-earth (RE) scandates, DyScO$_3$ and GdScO$_3$. They adopt an orthorhombic structure (*Pnma* space group), which derives from the ideal perovskite structure through an anti-phase tilting of the adjacent ScO$_6$ octahedra ($a^-b^+a^-$ in Glazer's notation [3, 4]). RE scandates currently receive active research interest as potential high-k dielectric materials [14–19] and as substrate materials for the epitaxial growth of strained high quality perovskite-type thin films [20–25]. Beyond the well adapted unit cell parameters for growth of several perovskite oxides, the crystalline perfection and homogeneity of the DyScO$_3$ and GdScO$_3$ single crystals and the rather low dislocation density make scandate single crystals some of the best available substrates for the epitaxial growth of perovskite thin films [20]. Given the fact that thin film growth takes place at high temperature, information on the temperature-dependent behaviour such as phase transitions or thermal

---

[1] Author to whom any correspondence should be addressed.

expansion is of importance. A previous x-ray diffraction (XRD) study indicates no phase transition in the 25–1000 °C range, though the orthorhombicity decreases with increasing temperature [26]. It is however well known that subtle phase transitions in perovskites are often below XRD resolution or very difficult to detect [5, 27]. The thermal expansion coefficients of $DyScO_3$ and $GdScO_3$ were determined in this temperature range [26] but the phonon thermal behaviour, and thus the Grüneisen parameters, remain unknown.

In the following we will present an investigation of $DyScO_3$ and $GdScO_3$ single crystals by means of temperature-dependent Raman scattering. Raman spectroscopy, which probes zone-centre phonons, is known to be a versatile technique for the investigation of oxide materials, in particular for the detection of small structural distortions in perovskites [28–34], even when they are too subtle to be detected by diffraction techniques [30, 35]. Building on our previous room temperature Raman study of $DyScO_3$ and $GdScO_3$ [36], our study aims to investigate the phonon spectrum up to 1200 °C, namely in view of a possible phase transition. To the best of our knowledge, this is the first temperature-dependent phonon investigation of any RE scandate.

2. Experimental details

$DyScO_3$ and $GdScO_3$ single crystal platelets supplied by *CrysTec* [37] have been investigated by Raman spectroscopy up to 1200 °C, using a commercial Linkam heating stage (TS1500) placed under the Raman microscope. Raman spectra were collected using a Jobin Yvon/Horiba LabRam spectrometer equipped with a liquid nitrogen cooled charge coupled device detector. Experiments were conducted in the micro-Raman mode in a backscattering geometry; the instrumental resolution was 2.8 ± 0.2 cm^{-1}. The 514.5 nm line of an Ar$^+$ ion laser was used as the excitation line for recording $DyScO_3$ spectra. For the investigation of $GdScO_3$ we used the 632.8 nm line of an He–Ne laser in order to limit the recently reported fluorescence, which almost entirely masks the phonon signature [36]. Experiments were carried out with a laser power below 5 mW on the sample. The light was focused to a 1 μm^2 spot using a 50× long working distance objective. Spectra were recorded every 50 °C in the range from room temperature up to 1200 °C for $DyScO_3$ and 1050 °C for $GdScO_3$ with an acquisition time varying between 50 and 100 s. Spectra were calibrated using the Si spectrum at room temperature. The Raman spectra before and after heating are identical, attesting to the reversibility of temperature-induced changes. The fitting procedure of the Raman lines was performed using the Labspec software of Horiba/Jobin Yvon by using Lorentzian profiles after subtraction of the baseline.

3. Results and discussion

3.1. Raman spectra

Before presenting the experimental Raman investigation, we recall that the primitive unit cell of the cubic perovskite
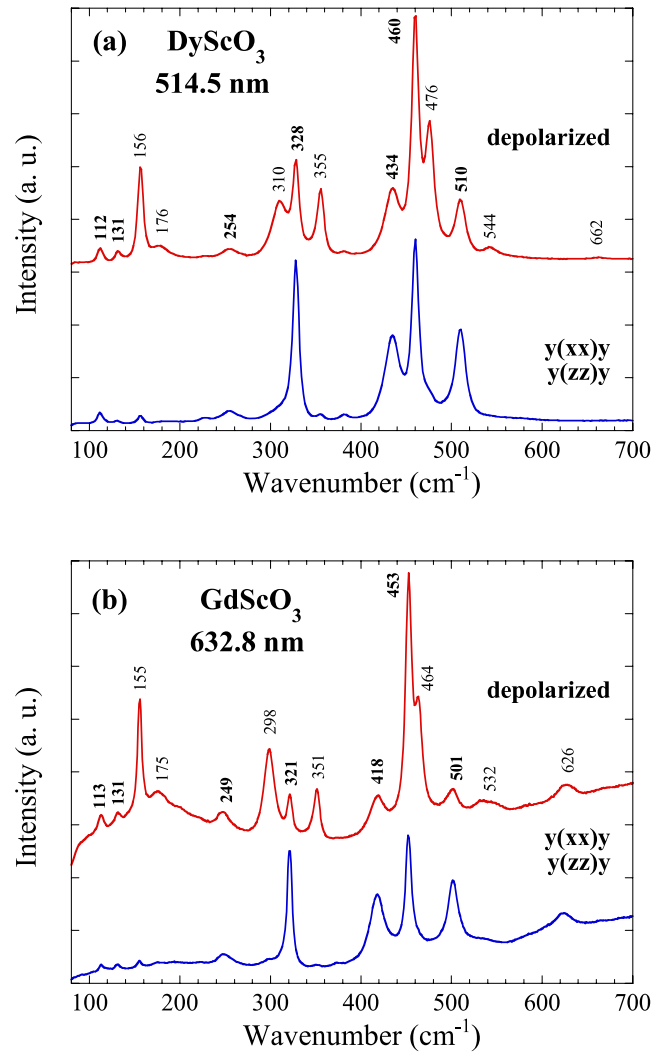

Figure 1. Raman spectra of (a) $DyScO_3$ and (b) $GdScO_3$ in both the unpolarized configuration and the parallel (VV) polarization configuration (orthorhombic reference setting ($y(xx)y$ or $y(zz)y$)). The A_g mode positions are given in bold.

contains one formula unit ABX_3 giving rise to 15 vibrational modes at the zone centre, which decompose into the following optical phonons: $\Gamma_{Pm\bar{3}m}(\text{opt}) = 3F_{1u} + F_{2u}$, where F_{1u} modes are IR active and F_{2u} is a silent mode and none of them are Raman active. On the other hand, the four $REScO_3$ formula units (thus 20 atoms) per unit cell in the orthorhombic *Pnma* structure, give rise to 60 vibrational modes at the zone centre, as predicted from factor group analysis: $\Gamma_{Pnma}(\text{opt}) = 7A_g + 5B_{1g} + 7B_{2g} + 5B_{3g} + 8A_u + 9B_{1u} + 7B_{2u} + 9B_{3u}$, whereof 24 modes are Raman active ($7A_g + 5B_{1g} + 7B_{2g} + 5B_{3g}$), 25 modes are IR active ($9B_{1u} + 7B_{2u} + 9B_{3u}$) and 8 modes are silent ($8A_u$). In a previous work we have reported polarized Raman spectra at room temperature, leading to the assignments of 23 modes out of the 24 predicted modes [36]. The experimental band positions for $DyScO_3$ are for most bands in reasonable agreement with recent theoretical *ab initio* predictions of the vibrational spectrum for the same material [18].

The temperature-dependent Raman experiments on $DyScO_3$ and $GdScO_3$ presented here have been carried out in
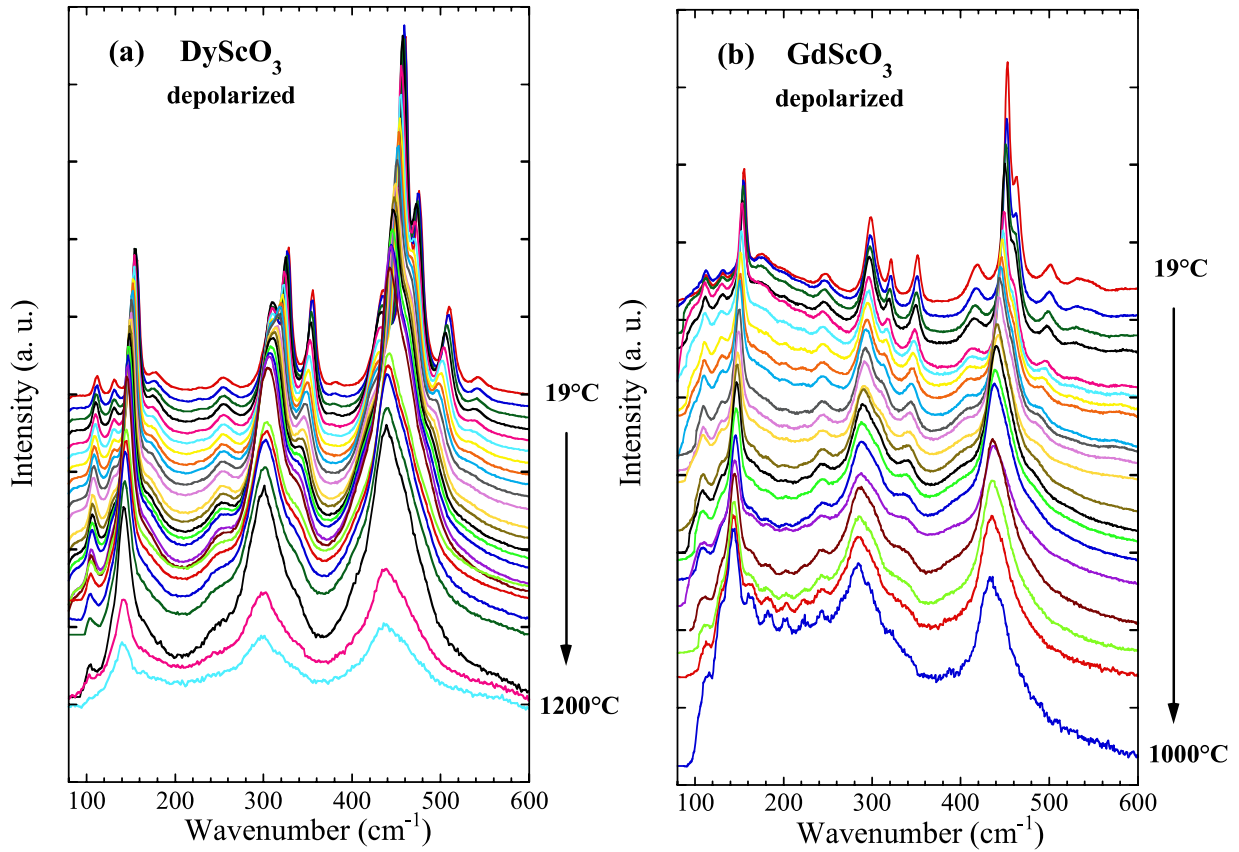
Figure 2. Temperature-dependent depolarized Raman spectra of (a) DyScO$_3$ and (b) GdScO$_3$.

two different configurations (see [36] for notation with respect to crystal orientations): in a first experiment, spectra have been recorded without polarization analysis; this configuration led to spectra which are rather similar to those obtained in the parallel polarization configuration $y(x'x')y$ or $y(z'z')y$ in the pseudo-cubic reference setting and contain mainly A$_g$ and B$_{2g}$ modes. A second experiment has been carried out in a configuration of parallel (VV) polarizer and analyser ($y(xx)y$ or $y(zz)y$ in the orthorhombic reference setting, i.e. after 45° rotation of the crystal platelets). In this parallel configuration only modes of A$_g$ symmetry are expected. Figures 1(a) and (b) present Raman spectra obtained at room temperature for DyScO$_3$ and GdScO$_3$, respectively, in both configurations of polarization. Although the VV spectra are very similar to our previously reported data [36], we observe, further to the predicted intense A$_g$ modes, some weak modes of B$_{2g}$ and B$_{1g}$ symmetry also, which is probably due to a slight sample disorientation.

   Temperature-dependent Raman spectra of DyScO$_3$ and GdScO$_3$ are presented in figures 2(a) and (b) and in figure 3. It can be seen that the temperature evolutions of depolarized phonon spectra are rather similar for the two compounds. At high temperature the spectra are first disturbed and then masked by an increasing thermal black body radiation, which has inhibited measurements above 1200 °C. As expected, the Raman spectra of GdScO$_3$ which are recorded using a 633 nm excitation are disturbed earlier (starting at 750 °C) than the DyScO$_3$ spectra recorded at 514 nm (starting at 950 °C).
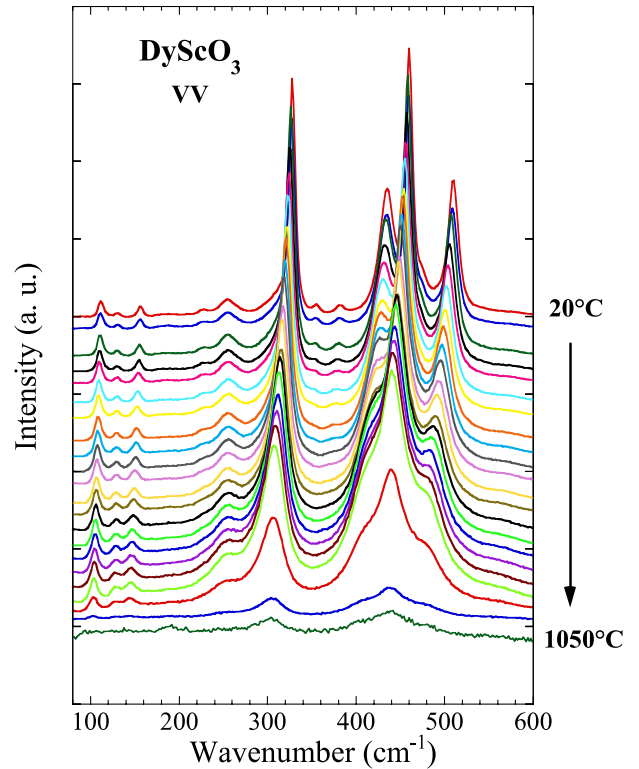

Figure 3. Temperature-dependent VV-polarized Raman spectra of DyScO$_3$. The intensity of the spectrum at 1050 °C is multiplied by a factor of 5.
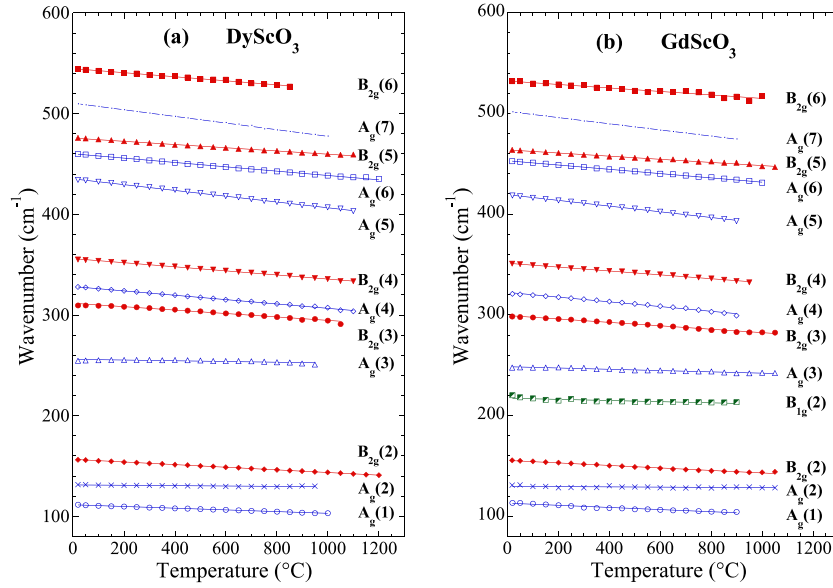
Figure 4. Temperature dependence of the positions of the well-defined Raman modes in (a) DyScO$_3$ and (b) GdScO$_3$. The lines are linear curve fits in the temperature range investigated.
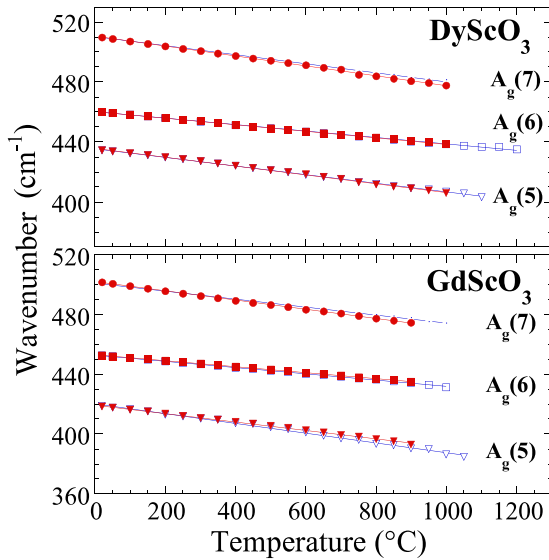

Figure 5. Temperature dependence of the positions of the three A$_g$ modes at high wavenumber of DyScO$_3$ and GdScO$_3$ collected in the two different polarization configurations (full symbols for polarized spectra, open symbols for depolarized spectra).

Further to this, the very high temperature GdScO$_3$ spectra are disturbed by unexplained optical interference fringes below 240 cm^{-1}. As expected, all Raman lines shift towards low wavenumbers and broaden with increasing temperature. The fact that the spectral signature evolves continuously without suppression or appearance of new bands suggests that DyScO$_3$ and GdScO$_3$ undergo no phase transition in the temperature range investigated.

Although not all bands can be fitted up to the highest temperature, mainly due to band broadening and in turn band overlap, most bands can be reliably fitted. Figures 4(a) and (b) present the quantitative temperature evolution of the band positions for DyScO$_3$ and GdScO$_3$, respectively. The positions of modes collected in the two different polarization configurations are very close, as illustrated in figure 5 for the three A$_g$ modes at high wavenumber. With increasing temperature, all modes decrease monotonically in wavenumber without any anomaly, which again attests to the absence of a structural phase transition. As seen in table 1, the slopes from linear curve fits for each mode are rather similar for the two compounds. The modes can be classified into three types depending upon the slope values. A$_g$ modes observed below 300 cm^{-1} shift slowly (-0.15 to -1.05 cm^{-1}/100 °C) whereas, above 300 cm^{-1}, the shift is much faster (-2.1 to -3.3 cm^{-1}/100 °C). The B$_{1g}$(2) mode measured up to 900 °C for GdScO$_3$ shifts slowly (-0.59 cm^{-1}/100 °C), similarly to the A$_g$ modes below 300 cm^{-1} and to the 176 cm^{-1} mode in DyScO$_3$ (mode not assigned in [36]). B$_{2g}$ modes are situated in an intermediate zone (-1.2 to -2.0 cm^{-1}/100 °C).

It is interesting to note that the very high temperature spectra of DyScO$_3$ and GdScO$_3$ can be qualitatively described in terms of three broad features, although the fine structure modes are still needed for the fit up to the highest temperature. The three broad features are approximately centred at 142, 301, 441 cm^{-1} and 145, 288, 439 cm^{-1} for DyScO$_3$ and GdScO$_3$, respectively. Generally speaking, the tendency to reduce the number of bands points to an evolution towards a higher symmetry. The fact that we observe three large phonon features is reminiscent of the three expected infrared-active phonon modes in the ideal cubic $Pm\bar{3}m$ perovskite structure. While it is common to observe three bands in infrared spectra for a structure that approaches a metrically cubic cell [38], it is more surprising to observe such features in Raman spectroscopy. Nevertheless, we take the signature of the three dominating Raman features as a strong argument for a decreasing orthorhombic distortion with a structural evolution of DyScO$_3$ and GdScO$_3$ towards the cubic $Pm\bar{3}m$

Table 1. Positions in wavenumber, slope values of the linear curve fits in figure 4 and Grüneisen parameters γ for each well-defined Raman mode in DyScO$_3$ and GdScO$_3$. The Grüneisen constants were derived from equation (1) in the text, by using the volumetric thermal expansion values α_V given in [26] ($\alpha_V = 2.42 \times 10^{-5}$ K^{-1} for DyScO$_3$ and $\alpha_V = 3.07 \times 10^{-5}$ K^{-1} for GdScO$_3$).

Mode assignment	DyScO$_3$			GdScO$_3$		
	ω (cm^{-1}) at 20 °C	$\delta\omega/\delta T$ (cm^{-1}/100 °C)	γ	ω (cm^{-1}) at 20 °C	$\delta\omega/\delta T$ (cm^{-1}/100 °C)	γ
A$_g$(1)	111	−0.87	3.24	113	−1.05	3.03
A$_g$(2)	131	−0.19	0.60	131	−0.15	0.37
B$_{2g}$(2)	156	−1.3	3.44	155	−1.2	2.52
?	176	−0.89	2.09	—	—	—
B$_{1g}$(2)	—	—	—	223	−0.59	0.86
A$_g$(3)	254	−0.91	1.48	248	−0.63	0.83
B$_{2g}$(3)	309	−1.7	2.27	298	−1.7	1.86
A$_g$(4)	327	−2.2	2.78	321	−2.3	2.33
B$_{2g}$(4)	355	−2.0	2.33	351	−1.9	1.76
A$_g$(5)	434	−2.9	2.76	418	−2.8	2.18
A$_g$(6)	459	−2.1	1.89	452	−2.1	1.51
B$_{2g}$(5)	475	−1.6	1.39	463	−1.5	1.06
A$_g$(7)	509	−3.3	2.68	501	−3.1	2.02
B$_{2g}$(6)	542	−2.0	1.53	532	−1.7	1.04

perovskite structure at high temperature. We then interpret the high temperature Raman signature as being dominated by thermal disorder (breaking the strict Raman selection rule). This tendency towards a cubic structure based on spectroscopic arguments is in good agreement with an earlier reported thermal expansion study of DyScO$_3$ and GdScO$_3$ using XRD [26]. In order to estimate the critical temperature at which an orthorhombic-to-cubic phase transition could take place, we have extrapolated the linear fit of the modes to higher temperatures to identify their point of intersection. Results (not shown here) indicate that three couples of A$_g$ and B$_{2g}$ modes intersect at very high temperatures. The lowest intersection temperature is found at approximately 2035 °C for B$_{2g}$(5) and A$_g$(7) for DyScO$_3$ and 2320 °C for A$_g$(2) and B$_{2g}$(2) for GdScO$_3$. These temperatures are close to or higher than the melting point for both rare-earth scandates ($\cong$ 2100 °C [20, 39]), which might exclude the possibility of the experimental observation of such a phase transition before melting.

3.2. Thermal expansion

The thermal expansion coefficients of DyScO$_3$ and GdScO$_3$ have been determined earlier from 25 to 1000 °C using XRD [26]. The calculated volumetric thermal expansion coefficients of DyScO$_3$ and GdScO$_3$ are $\alpha_{V,DSO} = 2.42 \times 10^{-5}$ K^{-1} and $\alpha_{V,GSO} = 3.07 \times 10^{-5}$ K^{-1}, respectively.

We have seen in section 3.1 that the frequency of all Raman modes decreases to a good approximation linearly with temperature from room temperature to 1200 °C. Such a linear temperature dependence makes the Raman modes themselves in principle suitable for the determination of the thermal expansion, assuming that changes in the volume, ΔV, and thus bond distances, Δd, induce changes in force constants and thus in vibrational frequencies. The Grüneisen model assumes that the Grüneisen constant γ correlates the temperature dependence of vibrational frequencies with the

unit cell volume. At constant pressure the Grüneisen constant is defined by

$$\gamma = \frac{\partial \ln \nu}{\partial \ln V}\bigg|_P = -\frac{1}{\alpha_V} \frac{\partial \ln \nu}{\partial T}\bigg|_P \qquad (1)$$

where ν is the frequency of a vibrational mode, V the unit cell volume and α_V the volumetric thermal expansion given by

$$\alpha_V = \frac{1}{V} \frac{\partial V}{\partial T}\bigg|_p. \qquad (2)$$

As a consequence, when the temperature dependence of vibrational modes is known, the Grüneisen parameter can be determined from the known thermal expansion (or vice versa). The so-calculated Grüneisen parameters are given in table 1 under the assumption that the same volumetric thermal expansion α_V can be used for every mode. As expected, the Grüneisen parameters vary significantly from one mode to the other.

It is interesting to recall that the values of α_V in [26] are based on the approximation [40] that α_V of a tilt-distorted ABO$_3$ perovskite can be empirically expressed as a decoupled combination of changes of the B–O bond length (thermal expansion $\alpha_{V,oct}$ of regular octahedra) and the tilting angle of BO$_6$ octahedral framework (thermal expansion α_ϕ) according to $\alpha_V = \alpha_{V,oct} + \alpha_\phi$. The thermal expansion is thus calculated by considering only the BO$_6$ octahedra, while the A–O bond is taken into account indirectly via α_ϕ. We note in parenthesis that such an approach is similar to the so-called polyhedral approach, based on comparative crystal chemistry and developed by Hazen and Finger, which has been shown to be useful in predicting elastic properties of a large number of solids [41, 42].

On the basis of the principle of such a polyhedra-type approach, it has been proposed that elastic properties such as thermal expansion or compressibility of perovskites can be estimated through the analysis of particular Raman modes, even without explicit knowledge of the Grüneisen

parameters [43–45]. In the following we will test this model by using our temperature-dependent Raman spectra of DyScO$_3$ and GdScO$_3$. The method described in detail in [43] is based on the following assumptions. (i) Changes in the lattice parameter *a* induce changes in force constants *k* and consequently in vibrational frequencies (Grüneisen model) and (ii) polyhedron stretching modes involve mainly one type of force constant and the thermal expansion (or compressibility) of the polyhedron is determined by these microscopic force constants. On the basis of these assumptions, the approximation of a pseudo-cubic structure and that the force constants obey an empirical law for ionic crystals as described in [46], Loridant *et al* [43] have proposed that the thermal expansion of a polyhedron can be described using the following empirical equation:

$$\alpha_V = \frac{1}{V}\frac{\partial V}{\partial T}\bigg|_p \cong -\frac{6}{13}\frac{1}{\nu}\frac{\Delta\nu}{\Delta T}. \qquad (3)$$

For testing this surprisingly simple empirical law we need to identify vibrational modes which are representative for the thermal expansion. The authors of [43] have suggested identifying modes that are representative of both BO$_6$ and AO$_{12}$ polyhedra, which are the constituent polyhedra of perovskites; it is however not straightforward to find in which way (parallel circuit or serial circuit) the polyhedral elastic values should be summed [43, 45, 47]. Following the discussion above and the approximations in [26, 40], we will consider only one mode which is characteristic of the ScO$_6$ octahedra vibrations: the high wavenumber A$_{1g}$(7) in-phase stretching mode of ScO$_6$ octahedra (assignment from [48]). As a stretching mode, this mode involves directly Sc–O force constants and its $\Delta\nu/\Delta T$ slope is characteristic of the response of the elastic system to the external parameter temperature. Furthermore, it has been shown [49] that the position in wavenumber of this mode is for orthorhombic *Pnma* perovskites directly related to the octahedra tilt angle according to the empirical relationship 23.5 cm^{-1}/deg. For the 509 cm^{-1} mode of DyScO$_3$ this relationship gives an octahedra tilt angle of 22° in good agreement with the value of 21° determined from XRD [50].

Applying equation (3) to the A$_{1g}$(7) mode leads to $\alpha_{V,DSO} = 2.99 \times 10^{-5}$ K^{-1} and $\alpha_{V,GSO} = 2.85 \times 10^{-5}$ K^{-1} which have to be compared to the XRD determined values [26] $\alpha_{V,DSO} = 2.42 \times 10^{-5}$ K^{-1} and $\alpha_{V,GSO} = 3.07 \times 10^{-5}$ K^{-1}. The good agreement suggests that the model and approximations of [43], and also the chosen mode, provide a valuable approach for a first rough estimation of the thermal expansion via Raman modes, namely for materials for which experimental XRD thermal expansion data are not reported. However, more work is needed for further testing (and eventually improving) this simple Raman-mode-based model.

4. Conclusion

We have presented a temperature-dependent Raman scattering investigation of DyScO$_3$ and GdScO$_3$ single crystals from room temperature up to 1200 °C. Within this temperature range the crystals undergo no structural phase transition, as attested to by the fact that all modes decrease monotonically in wavenumber without anomaly. The spectral evolution suggests a decreasing orthorhombic distortion towards the ideal cubic structure. However, a potential orthorhombic-to-cubic phase transition is close to, or higher than, the melting point for both rare-earth scandates ($\cong$2100 °C), which might exclude the possibility of the experimental observation of such a phase transition before melting. It is shown that the temperature-dependent shift of a specific Raman phonon can be used for a rough estimation of the thermal expansion, thus validating the model and approximations of [43].

References

[1] Rabe K M, Ahn C H and Triscone J-M 2007 *Physics of Ferroelectrics: A Modern Perspective* (Berlin: Springer)
[2] Kreisel J, Noheda B and Dkhil B 2009 *Phase Transit.* **82** 633
[3] Glazer A M 1975 *Acta Crystallogr.* A **31** 756
[4] Glazer A M 1972 *Acta Crystallogr.* B **28** 3384
[5] Mitchell R H 2002 *Perovskites: Modern and Ancient* (Ontario (C): Almaz Press)
[6] Scott J F 1974 *Rev. Mod. Phys.* **46** 83
[7] Fleury P A, Scott J F and Worlock J M 1968 *Phys. Rev. Lett.* **21** 16
[8] Guennou M, Bouvier P, Kreisel J and Machon D 2010 *Phys. Rev.* B **81** 054115
[9] Scott J F 1969 *Phys. Rev.* **183** 823
[10] Bouvier P and Kreisel J 2002 *J. Phys.: Condens. Matter* **14** 3981
[11] Samara G A, Sakudo T and Yoshimitsu K 1975 *Phys. Rev. Lett.* **35** 1767
[12] Angel R J, Zhao J and Ross N L 2005 *Phys. Rev. Lett.* **95** 025503
[13] Tohei T, Kuwabara A, Yamamoto T, Oba F and Tanaka I 2005 *Phys. Rev. Lett.* **94** 035502
[14] Schlom D G and Haeni J H 2002 *MRS Bull.* **27** 198
[15] Lim S-G, Kriventsov S, Jackson T N, Haeni J H, Schlom D G, Balbashov A M, Freeouf J L and Lucovsky G 2002 *J. Appl. Phys.* **91** 4500
[16] Lucovsky G, Zhang Y, Whitten J L, Schlom D G and Freeouf J L 2004 *Microelectron. Eng.* **72** 288
[17] Lucovsky G, Hong J G, Fulton C C, Zou Y, Nemanich R J, Ade H and Schlom D G 2004 *Phys. Status Solidi* b **241** 2221
[18] Delugas P, Fiorentini V, Filippetti A and Pourtois G 2007 *Phys. Rev.* B **75** 115126
[19] Christen H M, Jellison G E, Ohkubo I, Huang S, Reeves M E, Cicerrella E, Freeouf J L, Jia Y and Schlom D G 2006 *Appl. Phys. Lett.* **88** 262906
[20] Uecker R, Velickov B, Klimm D, Bertram R, Bernhagen M, Rabe M, Albrecht M, Fornari R and Schlom D G 2008 *J. Cryst. Growth* **310** 2649
[21] Haeni J H *et al* 2004 *Nature* **430** 758
[22] Choi K J, Biegalski M, Li Y L, Sharan A, Schubert J, Uecker R, Reiche P, Chen Y B, Pan X Q, Gopalan V, Chen L-Q, Schlom D G and Eom C B 2004 *Science* **306** 1005
[23] Vasudevarao A, Kumar A, Tian L, Haeni J H, Li Y L, Eklund C-J, Jia Q X, Uecker R, Reiche P, Rabe K M,

Chen L Q, Schlom D G and Gopalan V 2006 *Phys. Rev. Lett.* **97** 257602

[24] Catalan G, Janssens A, Rispens G, Csiszar S, Seeck O, Rijnders G, Blank D H A and Noheda B 2006 *Phys. Rev. Lett.* **96** 127602

[25] Wördenweber R, Hollmann E, Kutzner R and Schubert J 2007 *J. Appl. Phys.* **102** 044119

[26] Biegalski M D, Haeni J H, Trolier-McKinstry S, Schlom D G, Brandle C D and Graitis A J V 2005 *J. Mater. Res.* **20** 952

[27] Catalan G 2008 *Phase Transit.* **81** 729

[28] Zhang P, Haage T, Habermeier H-U, Ruf T and Cardona M 1996 *J. Appl. Phys.* **80** 2935

[29] Thomsen C, Wegerer R, Habermeier H U and Cardona M 1992 *Solid State Commun.* **83** 199

[30] Zaghrioui M, Bulou A, Lacorre P and Laffez P 2001 *Phys. Rev.* B **64** 081102

[31] Kreisel J, Pignard S, Vincent H, Senateur J P and Lucazeau G 1998 *Appl. Phys. Lett.* **73** 1194

[32] Kreisel J, Lucazeau G, Dubourdieu C, Rosina M and Weiss F 2002 *J. Phys.: Condens. Matter* **14** 5201

[33] Tenne D A, Gonenli I E, Soukiassian A, Schlom D G, Nakhmanson S M, Rabe K M and Xi X X 2007 *Phys. Rev.* B **76** 024303

[34] Pruzan P, Gourdain D and Chervin J C 2007 *Phase Transit.* **80** 1103

[35] Girardot C, Kreisel J, Pignard S, Caillault N and Weiss F 2008 *Phys. Rev.* B **78** 104101

[36] Chaix-Pluchery O and Kreisel J 2009 *J. Phys.: Condens. Matter* **21** 175901

[37] Crystec, Kristall-Technologie http://www.crystec.de/crystec-e.html

[38] Kamba S, Nuzhnyy D, Savinov M, Sebek J, Petzelt J, Prokleska J, Haumont R and Kreisel J 2007 *Phys. Rev.* B **75** 024403

[39] Wilke H, Crnogorac N and Cliffe K A 2007 *J. Cryst. Growth* **303** 246

[40] Zhao Y and Weidner D J 1991 *Phys. Chem. Miner.* **18** 294

[41] Hazen R M 1985 *Rev. Mineral.* **14** 317

[42] Hazen R M and Finger L W 1982 *Comparative Crystal Chemistry* (New York: Wiley)

[43] Loridant S and Lucazeau G 1999 *J. Raman Spectrosc.* **30** 485

[44] Chemarin C, Rosman N, Pagnier T and Lucazeau G 2000 *J. Solid State Chem.* **149** 298

[45] Kreisel J and Glazer A M 2000 *J. Phys.: Condens. Matter* **12** 9689

[46] Zallen R and Slade M L 1978 *Phys. Rev.* B **18** 5775

[47] Cornelius A L, Klotz S and Schilling J S 1992 *Physica* C **1992** 209

[48] Iliev M N, Abrashev M V, Lee H G, Popov V N, Sun Y Y, Thomsen C, Meng R L and Chu C W 1998 *Phys. Rev.* B **57** 2872

[49] Iliev M N, Abrashev M V, Laverdière J, Jandl S, Gospodinov M M, Wang Y-Q and Sun Y-Y 2006 *Phys. Rev.* B **73** 064302

[50] Velickov B, Kahlenberg V, Bertram R and Bernhagen M 2007 *Z. Kristallogr.* **222** 466